NASA DEVELOP National Program
California – JPL

Summer 2023

Southeast Coast Ecological Conservation

Investigating the Development of Ghost Forests Due to Saltwater Intrusion along the Savannah River, Georgia Coastline of the United States

DEVELOP Technical Report
August 11th, 2023

Emma Cheriegate (Project Lead)
Eleri Griffiths
Quintin Munoz
Vivienne von Welczeck

Advisors:
Dr. Elliot White Jr. (Stanford Woods Institute for the Environment, Stanford University)
Dr. Kyra Adams (NASA Jet Propulsion Laboratory, California Institute of Technology)
Benjamin Holt (NASA Jet Propulsion Laboratory, California Institute of Technology)

Fellow:
Michael Pazmino (JPL)

1. Abstract

Shallow aquifers along the southeastern US are experiencing saltwater intrusion from rising sea levels, changes in tidal cycles, and groundwater pumping, which are leading to higher soil salinity. Ghost forests, or areas where coastal forests have deteriorated due to salt water, are expanding in the Southeast US. We partnered with the USGS, USDA, and Georgia Southern University to investigate saltwater intrusion effects on coastal forests in the lower Savannah River using NASA Earth observation data spanning 2013 to 2023. The multi-sensor approach used Landsat 7 Enhanced Thematic Mapper Plus (ETM+), Landsat 8 Operational Land Imager (OLI), and Planet Labs' Dove PlanetScope & RapidEye Earth Imaging System (REIS). Our project aimed to determine the feasibility of detecting coastal forest health decline by creating a supervised land cover classification and analyzing the Normalized Difference Vegetation Index (NDVI). We directly linked a remote-sensing based time-series to in situ porewater salinity trends throughout the extent of the Savannah River. Our project ran at both a regional and site-level scale (4 USGS-monitored sites). We found differences in site-level NDVI values over 2013–2023 from both Landsat and Planet sensors. At the three sites nearest to the coast, we observed a muted seasonal variation that exhibited an inverse relationship with the increasing levels of river and porewater salinity found in those locations. The results provided here add to the growing body of research seeking to understand saltwater effects on coastal forests using spaceborne remote sensing and emphasize the need for proactive measures to mitigate saltwater intrusion's effects on coastal ecosystems.

Key Terms

Savannah River, Ghost Forests, Saltwater Intrusion, Coastal Ecosystems, NDVI, Land Cover Classification, Landsat 8, PlanetScope

2. Introduction

2.1 Background Information

Saltwater intrusion (SWI) is an increasingly prevalent phenomenon along global coasts. SWI has resulted in a visibly striking result: ghost forests, where once vibrant woodlands have been converted to marshland due to high influxes of saltwater. SWI poses a significant challenge to the coasts of the United States, where the Savannah River in Georgia's low-lying geography subjugates it to increasing rates of sea level rise and the intrusion of saltwater into its freshwater systems. Natural and anthropogenic factors drive SWI, including sea level rise, land subsidence, hurricanes or storm surges, subsequent flooding, and drainage systems (e.g., canals or ditches; Bhattachan et al, 2018; White and Kaplan, 2017). The resulting salinization affects soils, plants, and water bodies, particularly in low-lying coastal regions where rising sea levels exacerbate SWI further. As the freshwater boundary changes and saline water intrudes into a greater portion of the soil table, the regional flora health has been visibly impacted. This project investigated the extent of ghost forests, caused by increased soil salinity, as observed in a series of remotely sensed images from 2013 to 2023.

The use of satellite imagery in mapping and quantifying ghost forest extent is a relatively new venture, with the first reported attempt dating back to only 2021 (Ury et al., 2021). The authors employed a range of NASA Earth observations (EO), including atmospherically corrected Tier 1 Surface Reflectance images from 3 Landsat instruments: Landsat 5 Thematic Mapper (TM), Landsat 7 Enhanced Thematic Mapper Plus (ETM+), and Landsat 8 Operational Land Imager (OLI). They used Google Earth Engine (GEE) for land cover classification and a random forest algorithm to classify their inputs. However, while their choice of imagery and GEE bore similarity to the scope of this project, their penultimate aim of landcover classification does not. This project turned to vegetation indices and a salinity time series analysis, in addition to a land cover classification assessing the extent of ghost forests. The overarching goal of this work was to assess the feasibility of using NASA EO to identify ghost forests due to encroaching SWI.

The study area (Figure 1) lies primarily within the lower Savannah River Basin on the Georgia and South Carolina border. Adjacent to the Atlantic Ocean, this region is rich in biodiversity with a unique mosaic of coastal wetland ecosystems. While the Savannah River Watershed covers up to 27,000 km^2 (about the area of

New Jersey), the area of research focuses on the lower portion of the river (Wrona et al., 2007). This project defined the study area manually with satellite imagery and the Hydrologic Unit Code (HUC) 10 Watershed as a guide. We incorporated more of the coastline and upstream regions to gain a better understanding of the spatial differences along the Savannah River and surrounding areas.

In collaboration with the United States Geologic Survey (USGS) and the United States Department of Agriculture (USDA) partners, four USGS study plots that lie within the Savannah National Wildlife Refuge were selected for a more localized analysis. One study plot is about 26,000 feet (~5.0 miles) upstream from the three downstream plots. The upstream site is classified as a tidal freshwater forest at 32.2387°N, 81.1563°W. The three downstream plots are classified as moderately salt-impacted forest, heavily salt-impacted forest, and oligohaline marsh (Ensign et al., 2014). The study period for the project covers March 2013, to March 2023. Utilizing Earth observation imagery, the 10-year period captures mortality events due to natural factors such as hurricanes to monitor variables of interest over time.

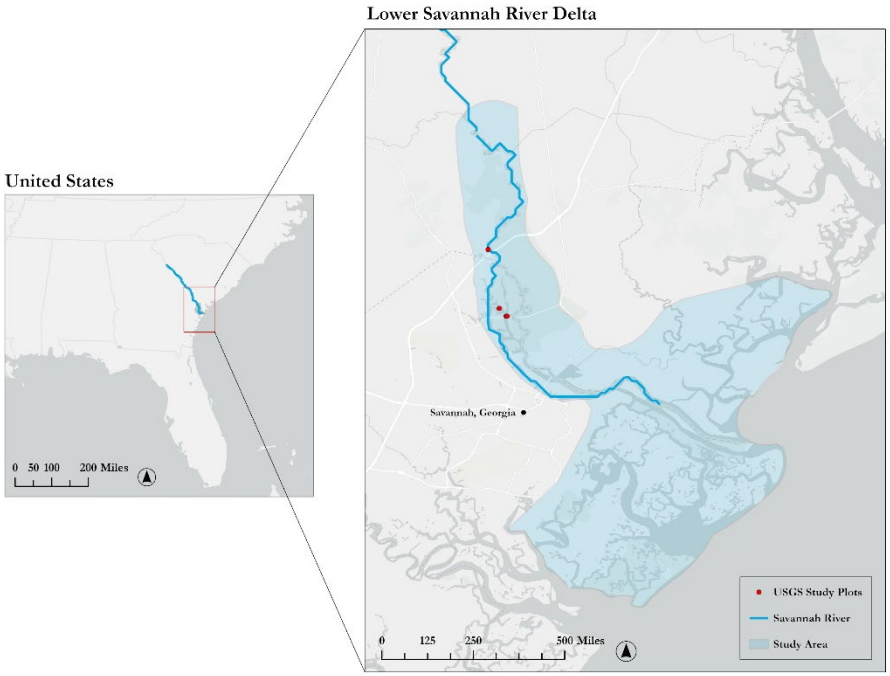

Figure 1. The study area for this project is located within the Lower Savannah Watershed. It encompasses four USGS study sites in the Savannah National Wildlife Refuge, which are located on the border of Georgia and South Carolina.

2.2 Project Partners & Objectives

The project partners include the Wetland and Aquatic Research Center (WARC) & the Florence Bascom Geoscience Center (FBGC) of the USGS, the Southeast Regional Climate Hub of the USDA, and Georgia Southern University (GSU). The researchers involved span a range of ecological, biogeochemical, and hydrological backgrounds. The WARC is a leader in aquatic ecosystem conservation, research, and management. The USDA is heavily invested in mitigating the future impacts of climate change, as evidenced by its launch of the Action Plan for Climate Adaptation and Resilience in 2021, a guide for Americans in the agriculture sector to aid in land management practices within a changing climate. The partners and collaborators of this project aid land managers with research in ecological forecasting, disaster prevention, and assessments. Their collective aspiration is to gain a deeper comprehension of the underlying factors and consequences associated with saltwater intrusions on local flora.

The objectives of this project focused on using NASA EO to identify ghost forest extent due to SWI along the Savannah River in the eastern region of Georgia, USA. Specifically, this project aimed to: 1) run a parallel process of Normalized Difference Vegetation Index (NDVI) calculations using sensors of different spatial resolutions to see if there is a difference reflected in the data; 2) create a land cover classification time series to understand land extent change over time; and 3) analyze porewater salinity trends throughout the extent of the Savannah River. To perform this comparison, linear regression analysis was applied to understand correlations between the datasets.

3. Methodology

3.1 Data Acquisition

The project team selected Landsat 7 ETM+ and Landsat 8 OLI via GEE as the NASA EOs used to evaluate the extent of ghost forests along the Savannah River Delta (Table 1). Landsat 8 OLI was selected as it contains data for the full duration of the study period, while Landsat 7 ETM+ was used as supplemental data to correct several outlier data points caused by cloud cover. For each of the Landsat sensors, we chose surface reflectance (SR) over top of atmosphere (TOA) reflectance for better imagery quality, as SR accounts for atmospheric distortions such as clouds and scattering (Vermote et al., 2016).

We also performed a parallel process with imagery from Planet's Dove PlanetScope & RapidEye Earth Imaging System (REIS) sensors to assess potential differences in results between sensors of different spatial resolutions. The imagery we selected for analysis from REIS were corrected surface reflectance images with 5 bands (Red, Green, Blue, Red Edge, & Near Infra-Red [NIR]) and corrected surface reflectance images with 4 bands (Red, Green, Blue, & NIR) for PlanetScope. REIS was chosen for the early portion of the study period as the Dove Constellation did not come online until 2014. From the Planet API we chose key images with the least amount of cloud coverage present, as restrictions limited the ability to apply a standardized cloud and water mask. The images selected were from the months of April 2013, April 2014, March 2015, and April 2023. Hereafter, the collection of PlanetScope and REIS imagery will be referred to as 'Planet Imagery'.

Our partners provided comprehensive in situ salinity data (monthly from 2013–2023) for four plot sites along the Savannah River in Georgia. Salinity data were utilized to verify and contrast the conclusions drawn from satellite images, offering important ground truth data that strengthened our research of the viability of using NASA EO to estimate the size of ghost forests. We acquired pertinent tide gauge data for the Fort Pulaski site (located at the river delta) from the National Oceanic and Atmospheric Administration (NOAA) to examine trends in sea level rise. This made it possible to comprehend how sea level rise plays a role in SWI.

Table 1
NASA EO datasets

EO	Resolution	Dates acquired	Data Product	DOI
Landsat 7 ETM+	30-meter	March 2013–June 2023	NASA Landsat 7 Enhanced Thematic Mapper Plus Sensor Collection 2 Level-1 Tier 1 Surface Reflectance and Surface Temperature	USGS EROS Archive - Landsat 7 Enhanced Thematic Mapper Plus (ETM+) Level-1 Data Products | USGS
Landsat 8 OLI	30-meter	March 2013–June 2023	NASA Landsat 8 Operational Land Imager and Thermal Infrared Sensor Collection 2 Level-2 Tier 1 Surface Reflectance	USGS EROS Archive - Landsat 8-9 OLI/TIRS Collection 2 Level-2 Science Products | USGS

Dove PlanetScope	3.25-meter	March 2021–April 2023	PlanetScope Basic Scene Level 1B, Surface Reflectance Product	Planet Monitoring - Satellite Imagery and Monitoring | Planet
RapidEye REIS	5-meter	March 2013–April 2015	RapidEye Scene Product	https://developers.planet.com/docs/data/rapideye/

3.2 Data Processing

3.2.1 Land Cover Classification

To examine the extent of coastal forest area in our region of interest (ROI; Figure 1) over our 10-year period, we utilized GEE and Landsat 8 OLI's atmospherically corrected Tier 1 surface reflectance product. All available scenes of the study area were clipped to the ROI. We applied a cloud mask to reduce cloud coverage obstructing the imagery, as well as a water and urban area mask generated from the National Landcover Database (NLCD) to ensure only coastal forest area was selected. We then created a seasonal composite from May to September to ensure our analysis focused on the growing season using 7 bands in total (coastal aerosol, blue, green, red, NIR, Short-wave Infra-Red [SWIR] 1, and SWIR 2).

3.2.2 Landsat NDVI

To gain deeper insight into temporal variations in vegetative health, our team performed an NDVI calculation using JavaScript API within the GEE platform. This API facilitated the examination of monthly NDVI trends over a span of 10 years within ROI. We initiated the analysis by importing spatial imagery from the USGS Landsat 8 Level 2, Collection 2, Tier 1 dataset, which was then clipped to the specified ROI. To reduce cloud cover obstruction, we applied a cloud mask. We then applied a water mask function using the Hansen global forest change dataset available within the GEE platform. Subsequently, we performed an NDVI calculation using relevant bands from the Landsat 8 sensor. The following NDVI formula was used (Huang et al., 2020):

$$NDVI = \frac{(NIR - Red)}{(NIR + Red)}$$

The resultant NDVI pixel values were then averaged for the selected month to generate a mean NDVI value for the entire month across the ROI. To obtain a comprehensive representation over the 10-year time period, we employed an iterate function to generate NDVI values for the subsequent 11 months, resulting in a total of 12 mean NDVI values for a complete annual cycle. Our script not only enables the spatial display of mean NDVI values for each month within the ROI but also facilitates the export of these values for further analysis. The same methodology was applied to the four USGS study sites with a 1-km buffer drawn around each site. This allowed us to compare mean monthly NDVI values across the four sites over the 10-year period.

3.2.3 Planet NDVI

We conducted a parallel analysis comparing NDVI data generated via high-resolution (3.5 & 5-meter) Planet imagery to (30-meter) Landsat imagery, to examine potential variations in NDVI values derived from imagery of varying spatial resolutions. The downloaded Planet images were stitched together as composites images from the growing season of the study period generated by PlanetScope and REIS sensors. Once the composite images were downloaded the images were processed using a custom GEE script that filtered out water pixels and performed an NDVI calculation to obtain the new NDVI imagery as well as NDVI values from the original composites.

3.2.4 Salinity Data

To analyze changes in porewater salinity over time, in situ data was provided by our USGS partners from four long-term USGS field sites along the Savannah River in the Savannah National Wildlife Refuge (see Table 2). Each site contained four wells that were sampled monthly. To analyze monthly changes within the

study period, we averaged the monthly salinity measurements for each well to create a new dataset with one average porewater salinity value per site per month. However, not all wells and months were sampled consistently throughout the study period. Months when sampling did not occur were represented with NA in this new dataset. Wells that did not have measurements within a month when sampling did occur were not included in the average calculation. This new dataset was then analyzed and visualized in RStudio 4.2.3 (Posit Team, 2023).

Table 2
USGS Long-Term Monitoring Sites

Site Number	*Site Name*	*Coordinates*	*USGS Land Classification*
1	SavUpper/Swamp 1	32.23863, -81.1563	Continuous freshwater tidal forest
2	Steamboat	32.17576, -81.1442	Moderately salt-impacted tidal forest
3	Rifle Cut	32.16722, -81.1368	Heavily salt-impacted forest
4	Rifle Cut Marsh	32.16728, -81.1359	Oligohaline marsh

3.3 Data Analysis

3.3.1 Supervised Land Cover Change Classification

We employed a Random Forest algorithm to train the supervised classification model. While multiple classification algorithms are readily available and often used, we decided on Random Forest for its reputation in outperforming Classification and Regression Tree (CART) in its ability to handle complex relationships and interactions between variables (Ury et al., 2021; Gislason et al., 2006). Random Forest worked by combining multiple decision trees to make predictions, utilizing a subset (70%) of the preprocessed training data with designated landcover classes (Marsh, Unhealthy Vegetation, Healthy Vegetation, and Evergreen), with the remaining (30%) training data used for an accuracy assessment. We trained the model by iteratively growing decision trees using manually delineated subsets (10 polygons containing 20 x 20 pixels) of the input features. The resulting decision trees were then used to classify the study area according to our landcover classes. Finally, we created a stacked animation of the 10 annual images, exemplifying how landcover extent has changed throughout our study region.

3.3.2 NDVI Parallel Processing using Landsat and Planet Data

When running a parallel analysis between Landsat and Planet imagery we hoped to see how the NDVI compared between the two sets of data at differing resolutions from 2013 to 2023. The spring growing season (March–June) was ultimately chosen when comparing the datasets. To compare Landsat and Planet datasets we employed two approaches for conducting the NDVI analysis: 1) by creating relative difference change detection maps for the whole regional study site and 2) by calculating the onsite NDVI values for the overall ROI as well as for USGS study plot sites.

3.3.2.1 Landsat Data

To further analyze the spatiotemporal differences across the ROI, we utilized the GEE script to export feature images for analysis. We extracted NDVI data for selected months, specifically June 2014 and June 2022, which were exported as GeoTIFF files and subsequently imported into ArcGIS Pro 3.1.0. By applying the change detection tool, we calculated the relative difference in pixel values between June 2022 and June 2014, comparing NDVI values across time and visualizing spatial changes in NDVI. A similar methodology was applied for the months of March 2023 and March 2013, as they offered improved image quality, lower cloud coverage, and lower NDVI values before the peak of growing season. In addition, the monthly mean NDVI values for each USGS study site were calculated for the duration of the study period and plotted graphically in RStudio using the ggplot2 package (Wickham, 2016) to visualize and compare trends between site locations.

3.3.2.2 Planet Data

To conduct the NDVI analysis on data derived from Planet, imagery was downloaded from Planet for specific key dates during the growing season of the study period, namely April 2013, April 2014, March 2015, and April 2023. Subsequently, the chosen images were imported into a custom script developed in GEE, tailored for processing Planet imagery. Once an image was imported and paired with a selected ROI, which could be the overall study site ROI or one of the four USGS plot site ROIs, the script was executed. The script's outputs consisted of an NDVI distribution image exported as a GeoTIFF for a given ROI, along with a corresponding numeric NDVI value associated with that same ROI. The NDVI GeoTIFF images were then utilized in subsequent processing steps to generate change detection maps. This was accomplished by applying the relative difference raster function using ArcGIS Pro. Additionally, the NDVI values were employed for further statistical analysis and the creation of data visualization graphics.

3.3.3 In Situ Data Analysis

We plotted Salinity data from the four USGS long-term monitoring sites (Table 2) in RStudio using the ggplot2 package (Wickham, 2016) to visualize changing trends across the project study period. We then ran the Pearson's correlation coefficient test on mean monthly NDVI and salinity values across all sites to determine the relative strength and direction of the association between these two variables. The Pearson's correlation coefficient ranges from -1 to 1, where a value of 1 indicates a perfect positive correlation or a direct relationship, 0 indicates no linear relationship, and -1 indicates a perfect negative correlation or an inverse relationship. By utilizing these correlation coefficients, we were able to identify and evaluate the significance of relationships between NDVI and porewater salinity.

4.1 Analysis of Results

4.1.1 Results of NDVI Calculations using Landsat 7 ETM+ and Landsat 8 OLI

At the regional scale, there was a slight difference in mean NDVI values between the mean of the first three years of the study period (0.346) compared to the final three years of the study period (0.337). The decrease is less than three percent and is difficult to interpret as numerous abiotic and biotic factors may contribute to differences in NDVI at the ROI scale over time. Figure 2 demonstrates the relative difference in NDVI between the months of March 2013 and 2023, as well as June 2014 and June 2022. These months were selected because they lie within the growing season and have minimal cloud coverage. Although we can assume most trees in the region reach maximum NDVI values by the end of June (Figure A1), a warmer climate across the globe is triggering a faster budburst date by up to 17 days (Jeong et al., 2013). The budburst date varies regionally across the globe but the deciduous vegetative cover within the Savannah River Delta follows a similar growth pattern across the 10-year scale based on the monthly mean NDVI graph. Figure A1 demonstrates an exponential rise in NDVI from April to June each year. After this initial jump in NDVI, the values stabilize until they decrease in fall through the winter dormant season.

ΔNDVI = March 2023 – March 2013

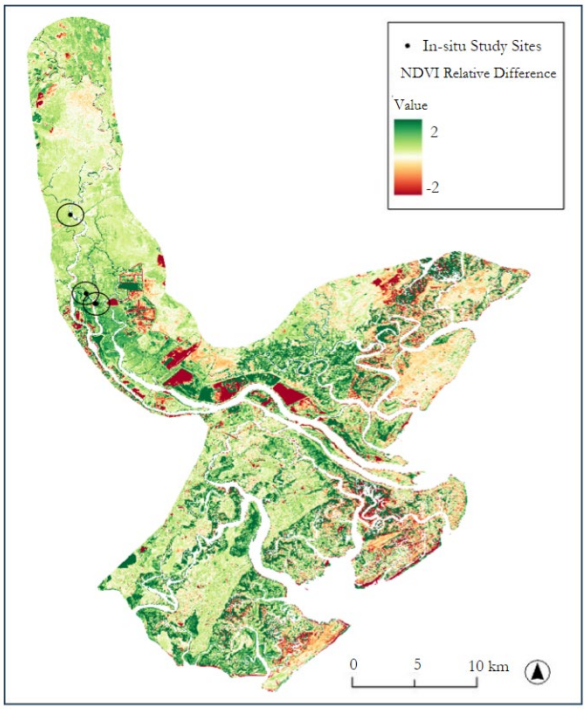

ΔNDVI = June 2022 – June 2014

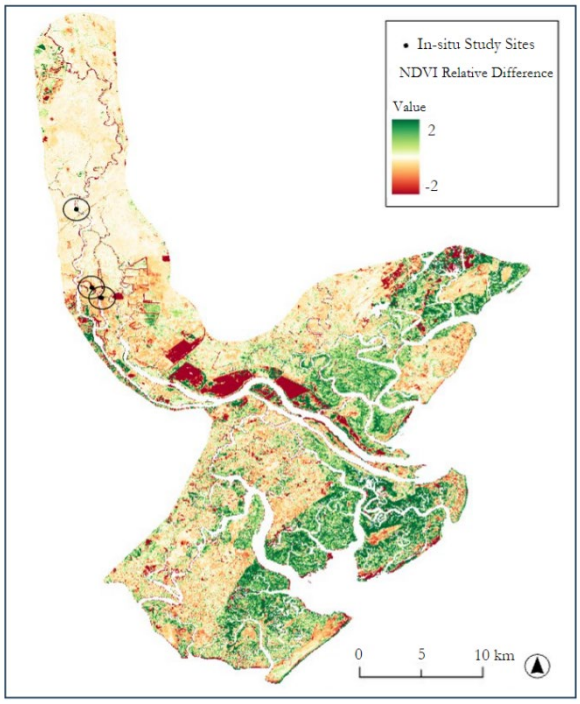

Figure 2: NDVI Relative Difference change detection using Landsat 7 ETM+ and Landsat 8 OLI sensor data. Pixel values with a white color indicate no change in NDVI while red and yellow indicate a negative decrease. Green values indicate a positive value of NDVI increase between the selected months.

We selected March because it captures the spatial extent of NDVI change before the exponential increase in the month of April. Figure 2 illustrates that the relative difference in March 2013 and 2023 reflect positive NDVI values. This is expected as the marsh landcover remains constant throughout the year, and deciduous vegetation has not fully budded. Following the month of April, however, the relative difference of June 2014 and 2022 in Figure 3, illustrates a greater spatial variation in NDVI values between early in the study period to more recent. Areas near the in situ study sites appear declining in vegetative health (especially those along the river) indicating vegetative stress.

For site specific NDVI values derived from Landsat over the 10-year period, Site 1 experienced a greater amount of seasonal variability in monthly mean NDVI values compared to Sites 2, 3, and 4 which display muted seasonal signals (Figure A1). We expected this outcome as Site 1 is further upstream and has less exposure to chronic SWI based on USGS porewater salinity measurements (see 4.1.4). The muted seasonal variation in sites 2, 3, and 4, highlights the significance of seasonal variability in coastal forests affected by SWI. This is driven by reduced canopy productivity during the growing season and additional understory vegetation which increases greenness in the dormant season (White & Kaplan, 2021).

4.1.2 Results of NDVI Calculations using Planet Imagery

ΔNDVI = April 2023 – April 2013 ΔNDVI = April 2023 – April 2014

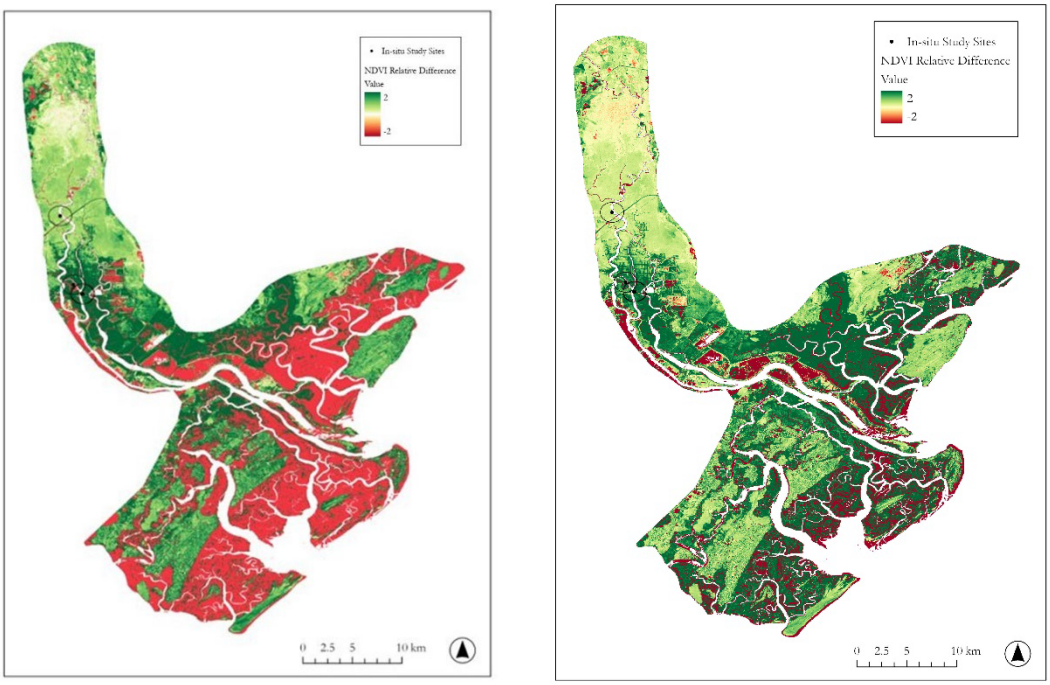

Figure 3: NDVI Relative Difference change detection using PlanetScope and REIS sensor data. The pixel values indicate the overall trend of NDVI per given study period, with pixel values in red indicating a decrease in NDVI and pixel values in green indicating an increase in NDVI for the entire region of interest. *Includes copyrighted material of Planet Labs PBC. All rights reserved.*

At the regional scale, a positive increase in NDVI was observed over the ten-year study period when using Planet imagery. This positive NDVI increase was observed both in creating the visual relative difference change detection maps and when calculating the numeric NDVI values for the ROI. The two images displayed in Figure 3 were outcomes of applying the relative difference raster function to Planet imagery. The resulting relative difference map shown on the left reflects the difference in NDVI for the entirety of the study period and was produced using Planet imagery from April 2013 and April 2023. The image depicts NDVI increases in green and decreases in red, overall indicating a fairly low NDVI increase for the 2013 to 2023 change detection image. Due to some challenges with resolution for 2013 imagery, an additional relative difference image was produced for April 2014 to April 2023. The outcomes of this relative difference detection are presented in the image on the right. In this case, a significant NDVI increase was observable on a region wide level especially when comparing the 2014 to 2023 relative difference image with the 2013 to 2023 image.

To further investigate the NDVI values reflected in the imagery, numeric NDVI values were also calculated at a regional scale. In the majority of cases, NDVI increased over the selected key years, with an NDVI value of 0.313 in 2013, 0.275 in 2014, 0.422 in 2015, and 0.527 in 2023. When assessing the magnitude of NDVI increase over the ten-year span, a difference computation was executed. To achieve this, the mean NDVI of the first three years of the study period was subtracted from the NDVI of the most recent year (2023). This method aimed to better highlight the observable fluctuations in NDVI over the ten-year span, which would have been less evident had the average of the whole ten-year span been used. The resultant mean NDVI value for the first three years was calculated as 0.338. Subtracting this mean NDVI value of 0.338 from the mean NDVI of 2023 (0.527) revealed an NDVI increase of 0.190 over the ten-year span for the overall ROI.

At the site level, a positive increase in NDVI was also observed over the ten-year period. When looking at the NDVI at the site level the analysis focused on the NDVI values generated for each of the four USGS plot sites per growing season of the key years 2013–2015 and 2023. The NDVI values observed at each USGS plot site are illustrated in Figure 4. A consistent increase in NDVI is evident across all four locations for each year. The data disclosed that the site furthest upstream (site one) consistently had the highest NDVI values over all four years, ranging from 0.50 in 2013 to 0.76 in 2023. The other three plot sites downstream exhibited a lower NDVI but similar in value, ranging from around 0.15 in 2013 and to around 0.50 by 2023.

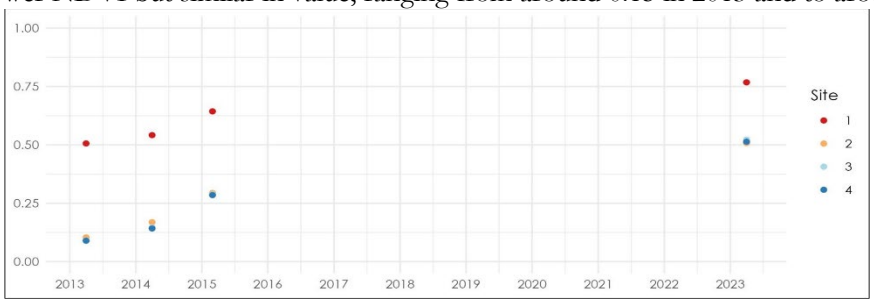

Figure 4: 2013–2015 & 2023 Planet NDVI values for USGS Plot Sites.

Just as one had calculated the NDVI difference for the overall ROI, the same approach was utilized in computing the NDVI difference per USGS plot site. After obtaining the NDVI values for each USGS plot site during the growing season of the key years of interest, the mean NDVI of the first three years was calculated and subtracted from the NDVI value of 2023 per plot site. This process yielded the mean difference value, as presented in Figure 5. The results of the difference calculation across all four USGS plot sites showed a mean NDVI increase across the board. The highest NDVI increase was recorded at site 3 in the middle section of the study area, with a NDVI difference of 0.347. Conversely, the lowest NDVI increase was observed at site 1, with a difference of 0.204.

Figure 5: Planet NDVI Plot Site Difference Calculation
(2023) NDVI – mean (2013, 2014, 2015) NDVI

The results of the parallel analysis between Landsat and Planet data were limited due to differing temporal and spatial resolutions between the instruments on the respective platforms, especially for the earlier part of the study period, most observable in 2013. While Planet data is acquired at a higher spatial resolution than Landsat data, less frequent flyovers at the start of the study period in 2013 accompanied by some API processing limitations (such as the lack of a standardized cloud and water mask) may have led to some notable differences when comparing NDVI values between the sensors. As Planet data became more consistent in 2014, there were more similarities between Landsat and Planet data. Overall, the parallel analysis between Landsat and Planet revealed site one to have the highest level of NDVI across all four years as well as similar NDVI values for sites two, three, and four where the monthly mean NDVI showed a more muted seasonal variability.

4.1.3. Results of Random Forest Land Cover Classification using Landsat 8 OLI

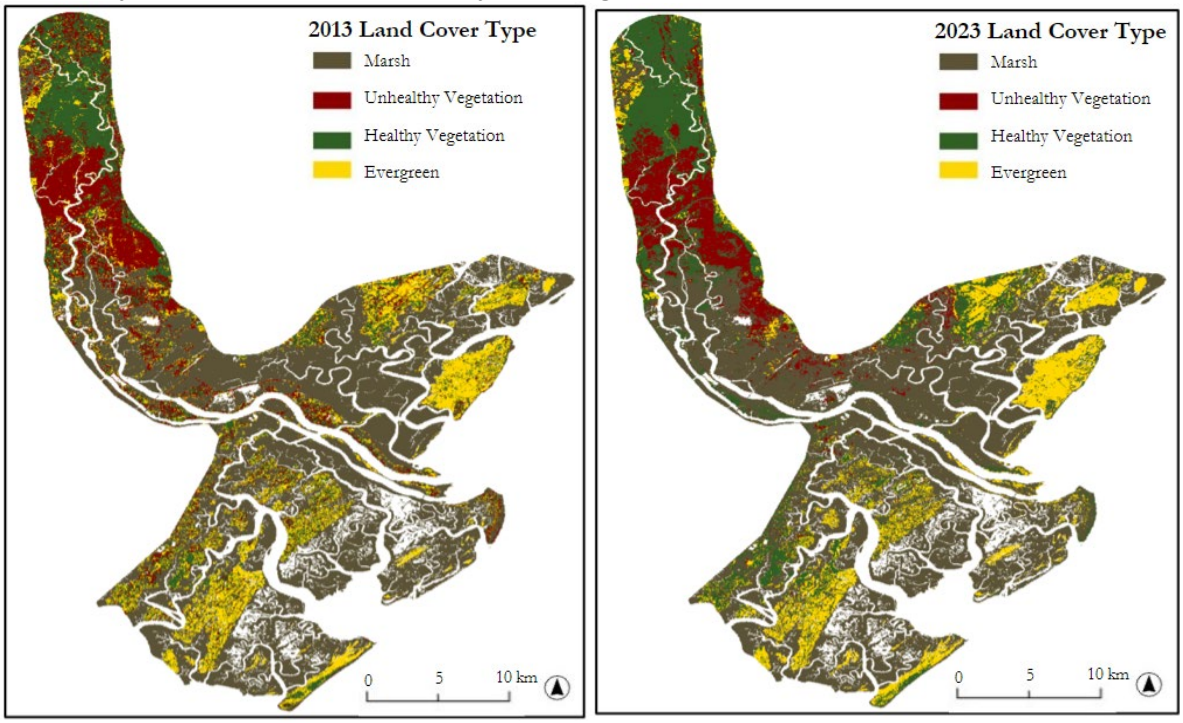

Figure 6: Land cover change detection using Landsat 8 OLI sensor data. The four designated classes are: Marsh, Unhealthy Vegetation, Healthy Vegetation, and Evergreen. Cloud, urban area, and water pixels were masked out to ensure only coastal forest area was selected.

We produced a total of 10 land cover change maps spanning the time period, serving as guides for partners to pinpoint potential areas of concern for further in situ investigation. Additionally, a time series analysis by area (in square meters) depicts the percentage-based alterations across the study duration (Table A2 in the appendix). The detailed tables A1 to A3 in the appendix present a more comprehensive detailing of land cover change data and model performance. We found the Evergreen class was the only class to experience an increase in total area and had the highest variability, suggesting the need for further investigation into complex hydrological conditions that could be influencing this outcome. Conversely, the other three classes—unhealthy vegetation, healthy vegetation, and marsh—experienced marginal declines in their overall areas (Table A2, Appendix). Notably, marsh area remained the most consistent and predominant class throughout the observed time span.

We observed classification accuracy (i.e., agreement with reference data) of 95–97 percent averages throughout the study years (Table A3). The 2013 and 2023 land cover maps created during this term (Figure 6) include a distinct shift in unhealthy vegetation and healthy vegetation in the northern portion of the ROI, which the USGS partners were especially interested in identifying, as it displays a potential shift in tidal influence. Ghost forests are notoriously difficult to map (White & Kaplan, 2021; Ury et al., 2021), as they present inherent difficulties in depicting distinct variations in land cover area. Due to time constraints, this land cover classification prioritized capturing broad trends in forest cover change rather than specific vegetation types. While we recognize this as a study limitation, we recommend that forthcoming land cover classifications encompass specific vegetation categorizations. Nonetheless, these maps and the time series analysis suggest that the data hold promise for exploratory studies investigating the extent of ghost forest land cover change, provided these limitations are considered.

4.1.4 Results of In Situ Data Analysis

NOAA tide gauge data for the Fort Pulaski gauge located at the mouth of the Savannah River estuary shows a clear increase in sea level rise throughout the study period (Figure A3). The rate of increase is almost 1 cm per year. This rapid rate of sea level rise could be due to the low-lying geography of this coastal region, which may exacerbate the effects of saltwater intrusion in this area, including porewater salinity levels at the four USGS sites included in this study.

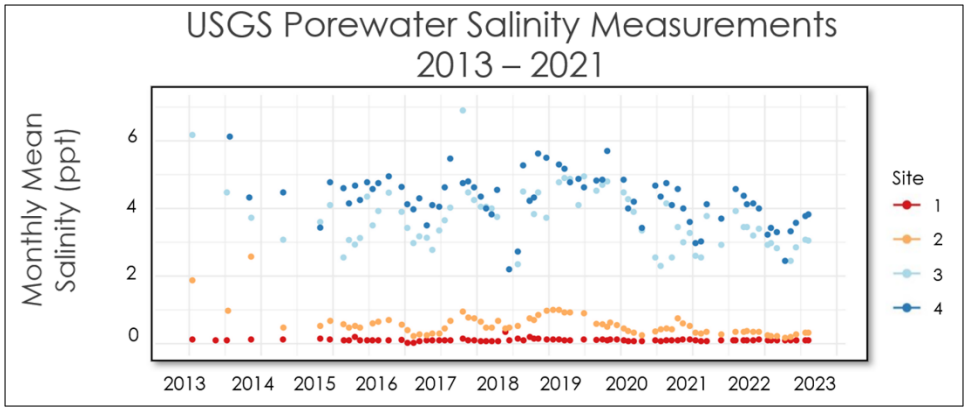

Figure 7: Porewater salinity measurements for the 4 USGS sites from 2013–2021.

In analyzing porewater salinity trends over time, average salinity increased by each site further downstream toward the coast (Figure 7). Site 1 had average salinity values close to zero parts per thousand (ppt) throughout the study period, Site 2 had salinity values ranging from 0.17 to 2.7 ppt, Site 3 salinity averages ranged from 2.30 to 6.90 ppt, and Site 4 had average salinity values from 2.20 to 7.02 ppt. While there does not seem to be a clear trend over time overall with porewater salinity across sites, the difference in salinity levels between sites correlates to the Landsat NDVI trends over time, with the downriver, more saline sites (Sites 3 and 4) exhibiting a more muted NDVI seasonal variability. Additionally, a Pearson's correlation coefficient test was conducted on the porewater salinity and Landsat NDVI values across all sites. The resulting correlation coefficient was –0.16 with a p-value of 0.005, indicating a significant negative relationship between salinity and Landsat NDVI on the site level. While there are a variety of drivers for NDVI seasonal variability, this observed trend and the significant negative correlation may be an indication of the long-term impacts of saltwater intrusion in this area of the river.

4.2 Feasibility Assessment & Limitations

The feasibility of this study hinged on the availability of clear imagery from both Landsat and Planet platforms. However, it is essential to acknowledge the challenges that emerged, significantly influencing the execution of the analysis. Both Landsat and Planet imagery were subject to constraints arising from the timing of satellite flyovers and cloud coverage. These variables exerted an impact on the frequency and quality of obtainable images, potentially introducing gaps in the temporal record and diminishing the accuracy of vegetation dynamics monitoring. On a parallel note, the Planet platform introduced its own set of feasibility concerns. During the initial years of the study period, a limitation in the number of flyover instances had ramifications on the availability of high-quality imagery. This could potentially distort the representation of vegetation dynamics during this phase. Processing complications stemming from the lack of accessible cloud mask code processing tools introduced an additional layer of challenge, possibly compromising the precision of data preprocessing and subsequent analysis.

The incorporation of both salinity levels and land cover classification also introduced their own limitations. While the correlation between salinity and vegetation health was evident, the salinity patterns might be limited by sparse data availability for the beginning of the study period. In addition, the porewater salinity analysis may have been influenced by sub-surface hydrological processes that are hard to detect by remote sensing. In terms of land cover classification, the effectiveness of the model could be limited by the number of training points employed. Despite manually delineating 10 training polygons (containing 20x20 pixels), the size of each (as well as Landsat 8's relatively coarser spatial resolution) could contribute to edge effects, obscuring the boundary between each class. In summary, this study grappled with a multitude of feasibility and limitations factors intrinsic to the utilization of varying NASA EO and Planet sensors for NDVI calculations, salinity data, and land cover classification. A careful and nuanced interpretation of the results is imperative, taking into account these complex challenges that inherently shape the outcomes of specific ecological analysis.

4.3 Future Work

Future work could include extending or adjusting the study period to capture more historical or recent trends (extending further into the past or looking at specific hurricane events), running multiple land cover classification algorithms and comparing results & accuracy, creating a classification based on specific tree species, and incorporating stream salinity in addition to porewater salinity measurements. This combined approach could offer a more comprehensive grasp of hydrological and groundwater dynamics, thereby contributing to a deeper understanding of the salinity trends. Additionally, examining the impact of factors such as land subsidence, groundwater extraction, sea level rise, and dredging on soil water infiltration could provide a deeper understanding of land cover dynamics under changing conditions. Pursuing these directions could enhance our insights into the complex relationships shaping vegetation patterns and soil-water interactions.

5. Conclusions

This study used Landsat 8 and Planet imagery to analyze the dynamics of vegetation health and land cover changes within the designated region of interest (ROI), comparing them to salinity measurements from 2013–2023. The observed disparity in NDVI trends between the two datasets highlights the significance of spatial resolution and imagery characteristics in influencing the calculated values. In assessing Landsat and Planet data, their divergent temporal and spatial resolutions, particularly evident in the earlier years like 2013, constrained our comparative analysis. Planet's higher spatial resolution was tempered by sporadic temporal coverage and API processing limitations during this period, resulting in discernible differences in NDVI values when compared to Landsat. Nevertheless, as Planet data consistency improved in 2014, alignment with Landsat results became more apparent. Despite these challenges, significant insights emerged: site one consistently displayed the highest NDVI levels throughout all four years, while sites two, three, and four exhibited similar, muted seasonal variability in monthly mean NDVI values. This underscores the value of integrating high or multi-resolution datasets for a comprehensive grasp of regional vegetation dynamics.

The stability of marshes and their prevalence in the ROI suggest their robustness in saline environments, possibly contributing to their consistent dominance. In contrast, the variability observed in evergreen areas exhibits the need for further investigation into the ecological implications of their increasing presence over time. By comparing on-site salinity measurements with NDVI values, a clear negative correlation emerged: as salinity increased, NDVI values decreased. This research contributes valuable insights into the intricate interactions between vegetation, land cover, and environmental factors at a regional scale, adding to a growing body of research on the complexity in SWI dynamics that shape the coastal ecosystems.

6. Acknowledgements

Project Partners:

- Dr. Steve McNulty, Southeast Regional Climate Hub (USDA)
- Michael Gavazzi, Southeast Regional Climate Hub (USDA)
- Dr. Gregory Noe, FBGC (USGS)
- Dr. Beth Middleton, WARC (USGS)
- Dr. Ken Krauss, WARC (USGS)
- Dr. Georgianne Moore, Chair Biology (Georgia Southern University)
- Dr. CJ Pell, postdoc (Georgia Southern University)

Special Thanks:

- Dr. Kyra Adams, NASA Jet Propulsion Laboratory, California Institute of Technology
- Dr. Elliott White Jr., Stanford Woods Institute for the Environment
- Benjamin Holt, NASA Jet Propulsion Laboratory, California Institute of Technology
- Michael Pazmino (JPL Node Fellow)
- Laramie Plott (Project Coordination Fellow)

Any opinions, findings, and conclusions or recommendations expressed in this material are those of the author(s) and do not necessarily reflect the views of the National Aeronautics and Space Administration. This material is based upon work supported by NASA through contract NNL16AA05C.

This work utilized data made available through the NASA Commercial Smallsat Data Acquisition (CSDA) program.

7. Glossary

CART – Classification and Regression Tree, a landcover classification algorithm
Earth observations (EO) – Satellites and sensors that collect information about the Earth's physical, chemical, and biological systems over space and time
ETM+ – Enhanced Thematic Mapper Plus
GEE – Google Earth Engine is a catalog of satellite imagery and geospatial datasets with planetary-scale analysis capabilities used to detect changes, map trends, and quantify differences on the Earth's surface.
NASA – National Aeronautics and Space Administration which is a United States government agency that is responsible for science and technology related to air and space.
NDVI – Normalized Difference Vegetation Index which quantifies vegetation by measuring the difference between near-infrared (which vegetation strongly reflects) and red light (which vegetation absorbs)
OLI – Operational Land Imager
ROI – Region of interest, or study area
SWI – Saltwater intrusion
TM – Thematic Mapper

8. References

Bhattachan, A., Emanuel, R. E., Ardón, M., Bernhardt, E. S., Anderson, S. M., Stillwagon, M. G., Ury, E. A., BenDor, T. K., & Wright, J. P. (2018). Evaluating the effects of land-use change and future climate change on vulnerability of coastal landscapes to saltwater intrusion. Elementa: Science of the Anthropocene, 6. https://doi.org/10.1525/elementa.316

Ensign, Scott H., et al. "Sediment Accretion in Tidal Freshwater Forests and Oligohaline Marshes of the Waccamaw and Savannah Rivers, USA." Estuaries and Coasts, vol. 37, no. 5, 2014, pp. 1107-1119. DOI: 10.1007/s12237-013-9744-7.

Gislason, P. O., Benediktsson, J. A., & Sveinsson, J. R. (2006). Random forests for land cover classification. Pattern Recognition Letters, 27(4), 294–300. https://doi.org/10.1016/j.patrec.2005.08.011

Huang, S., Hupy, J. P., Shao, G., Tang, L., Wang, Y. (2020). A commentary review on the use of normalized difference vegetation index (NDVI) in the era of popular remote sensing. Journal of Forestry Research, 32, 1-6. https://doi.org/10.1007/s11676-020-01155-1

Jeong, S.-J., Medvigy, D., Shevliakova, E., and Malyshev, S. (2013), Predicting changes in temperate forest budburst using continental-scale observations and models, Geophys. Res. Lett., 40, 359–364, doi:10.1029/2012GL054431.

Planet Team. (2017). Planet Application Program Interface: In Space for Life on Earth. San Francisco, CA. https://api.planet.com/.

Posit Team (2023). RStudio: Integrated Development Environment for R. Posit Software, PBC, Boston, MA. http://www.posit.co/

United States Geological Survey, Earth Resources Observation and Science Center. (2021). Landsat 7 ETM Plus Collection 2 Level-2 Science Products [Data set] U.S. Department of the Interior. https://doi.org/10.5066/p9c7i13b

United States Geological Survey, Earth Resources Observation and Science Center. (2021). Landsat 8. OLI/TIRS Level-2 Data Products - Surface Reflectance [Data set] U.S. Department of the Interior. https://doi.org/10.5066/f78s4mzj

Ury, E. A., Yang, X., Wright, J. P., & Bernhardt, E. S. (2021). Rapid deforestation of a coastal landscape driven by sea-level rise and extreme events. Ecological Applications, 31(5). https://doi.org/10.1002/eap.2339

Vermote, E., Justice, C., Claverie, M., & Franch, B. (2016). Preliminary analysis of the performance of the Landsat 8/OLI land surface reflectance product. *Remote sensing of environment*, *Volume 185*(Iss 2), 46–56. https://doi.org/10.1016/j.rse.2016.04.008

White, E., & Kaplan, D. (2021). Identifying the effects of chronic saltwater intrusion in coastal floodplain swamps using remote sensing. Remote Sensing of Environment, 258, 112385. https://doi.org/10.1016/j.rse.2021.112385

White, E., & Kaplan, D. (2017). Restore or retreat? saltwater intrusion and water management in coastal wetlands. *Ecosystem Health and Sustainability*, *3*(1). https://doi.org/10.1002/ehs2.1258

Wickham, H. (2016). Ggplot2: Elegant Graphics for Data Analysis. Springer-Verlag New York. https://ggplot2.tidyverse.org

Wrona, A., Wear, D., Ward, J., Sharitz, R., Rosenzweig, J., Richardson, J.P., Peterson, D., Leach, S., Lee, L., Jackson, C.R., Gordon, J., Freeman, M., Flite, O., Eidson, G., Davis, M., & Batzer., D. (2007). Restoring Ecological Flows to the Lower Savannah River: A Collaborative Scientific Approach to Adaptive Management. Proceedings of the 2007 Georgia Water Resources Conference, pp. 538-549.

9. Appendices

Appendix A

Table A1 *Land Cover Change classification scheme.*

Class ID	Landcover Type	Class Description
1	Marsh	Classified as waterlogged areas characterized by emergent vegetation, offering a habitat for various aquatic plants and wildlife.
2	Unhealthy Vegetation	Classified as areas with stressed, degraded, or visually dead vegetation.
3	Healthy Vegetation	Classified as areas vibrant and robust vegetation cover, indicating a balanced and flourishing ecosystem.
4	Evergreen Forest	Areas dominated by trees generally on higher elevation, pine and oak predominate.

Table A2
Percentage of area (m^2) for each class throughout the 10-year study period (2013–2023)

Year	Marsh	Unhealthy Vegetation	Healthy Vegetation	Evergreen
2013	56.8	10	17.2	16.1
2014	61.1	10.3	11.8	16.8
2015	55.5	9.9	11.2	23.4
2016	53.6	9.9	12.1	24.4
2017	60.8	9.2	15	15
2018	63	10.1	12.8	14.1
2019	62.8	10.1	9.5	17.6
2020	66.5	10.3	10.1	13.1
2021	60.2	8.9	12.8	18.1
2022	52.6	10.2	11.9	25.3
2023	51.4	9.2	12.3	27.1

Table A3
Overall accuracy assessment error matrix for 2013–2023 Land Cover Change classification (averaged between all years)

Class	Total # of Points per Class	Producer's Accuracy	User's Accuracy	Kappa Coeff.
Marsh	10, 20x20 pixels each	0.98	0.97	0.96
Unhealthy Vegetation	10, 20x20 pixels each	0.98	0.96	0.96
Healthy Vegetation	10, 20x20 pixels each	0.94	0.95	0.96
Evergreen Forest	10, 20x20 pixels each	0.96	0.97	0.96

Figure A1

Monthly Mean NDVI values over a 10-year period between all four USGS study sites. The sites are in order with site 1 furthest upstream and site 4 downstream. Each site has a 1-kilometer circular buffer zone.

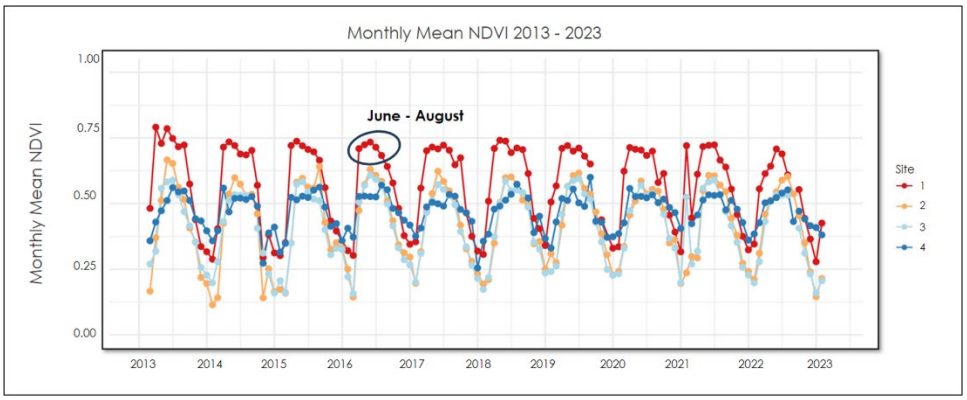

Figure A2

Land cover time series showing the percentage area (square meters) changed over the 10-year study period.

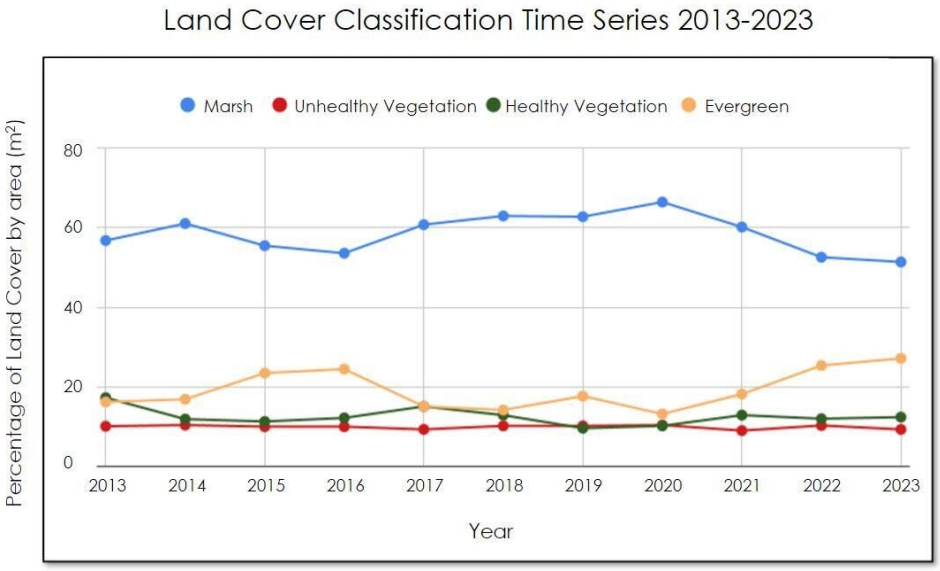

Figure A3

Tide gauge levels for Fort Pulaski gauge (closest to the coast) show a dramatic increase in sea level from 2013–2023.